ical curve with the experimental points, the ratio of the observed radiative capture probability to the theoretically calculated one was found to be 1.10 ± 0.25.

ACKNOWLEDGMENTS

The writer wishes to express appreciation for the kind interest of Dr. C. E. Mandeville who prepared this manuscript for publication. Useful discussions with Dr. F. R. Metzger are also gratefully acknowledged. The various chemical purifications were performed by Dr. W. B. Keighton of Swarthmore College. The author wishes to further express appreciation for the award of a fellowship by the Bartol Research Foundation, and to Dr. W. F. G. Swann for encouragement.

PHYSICAL REVIEW VOLUME 102, NUMBER 2 APRIL 15, 1956

Elastic Scattering of 340-Mev Protons by Deuterons*

OWEN CHAMBERLAIN AND DAVID D. CLARK†
Department of Physics and Radiation Laboratory, University of California, Berkeley, California
(Received December 19, 1955)

The differential cross section for the elastic scattering of 340-Mev protons by deuterons has been measured at eight angles from 30° to 150° in the center-of-mass system. A coincidence counting system using scintillation counters detected both product particles, the elastic effect being separated from the inelastic through identification of the scattered deuterons by photographically recorded pulse heights produced in a counter telescope. The resulting cross section is, at 30°, 2.2 mb/steradian; 40°, 0.89; 50°, 0.39; 70°, 0.11; 90°, 0.047; 110°, 0.042; 130°, 0.047; and 150°, 0.099, in center-of-mass units. The total (statistical and systematic) errors range from 15 to 24%. The total elastic cross section is estimated to be 6.0 ± 1.2 mb. Problems of interpretation using the impulse approximation are discussed; the sticking factor is calculated for three different *n-p* potentials. At scattering angles of 30° and 40° there appears to be very little interference effect between *n-p* and *p-p* scattering. The interference is perhaps slightly destructive.

I. INTRODUCTION

THE role of nucleon-deuteron scattering in the attempt to learn more about nuclear forces is threefold. First, it gives data on the scattering of nucleons by a simple nuclear system. Second, we expect that between the scattered waves from the two components of the deuteron there will be interference effects that will give us information as to the relative phases of the nucleon-nucleon scattering amplitudes. Third, as targets consisting of neutrons do not exist, neutron-deuteron scattering is our closest approach to *n-n* scattering, and a comparison of *n-d* and *p-d* scattering can answer the question of whether or not nuclear forces are charge-symmetric. Moreover, though nucleon-deuteron scattering is a three-body problem, theoretical treatment—at least for small angles of deflection—is possible at the higher energies by use of the impulse approximation.

Experimental work to date in the higher energy region has been that of Ashby[1] (32-Mev *p-d* scattering; 21 Mev available in the center-of-mass system); Chamberlain and Stern[2] (192-Mev *d-p*; 63 Mev in c.m. system); Cassels, Stafford, and Pickavance[3] (145-Mev *p-d*; 95 Mev in c.m. system); and Schamberger[4] (240-Mev *p-d*; 156 Mev in c.m. system). The 90-Mev *n-d* (59 Mev in c.m. system) case has been studied both by Powell[5] with cloud-chamber techniques and very recently by Youtz[6] with counters. The pick-up region (near 180°) of *p-d* scattering has been the subject of Bratenahl[7] at energies from 95 to 138 Mev, and of Teem and Kruse[8] at 95 Mev.

The experiment described here was undertaken because of the usefulness of any additional high-energy scattering data, and in particular because the impulse approximation becomes increasingly valid with higher energy. The proton beam energy used was 340 Mev, the available energy in the center-of-mass system being 218 Mev.

II. GENERAL METHOD

The process of measuring the cross section consisted of the measurement of the four quantities: $D(\Theta)$, the number of elastic *p-d* scattering events observed per

* This work was performed under the auspices of the U. S. Atomic Energy Commission. A portion of this research was submitted as a thesis by one of us (D.D.C.) in partial satisfaction of the requirements for the Ph.D. degree at the University of California.

† Now at Department of Engineering Physics, Rockefeller Hall, Cornell University, Ithaca, New York. For the major portion of this research, a U. S. Atomic Energy Commission predoctoral fellow.

[1] V. J. Ashby, University of California Radiation Laboratory Report UCRL-2091 (unpublished).

[2] O. Chamberlain and M. O. Stern, Phys. Rev. **94**, 666 (1954).

[3] Cassels, Stafford, and Pickavance, Nature **168**, 468 (1951).

[4] R. D. Schamberger, Phys. Rev. **85**, 424 (1952).

[5] W. Powell, University of California Radiation Laboratory Report UCRL-1191 (unpublished).

[6] B. L. Youtz, University of California Radiation Laboratory Report UCRL-2307 (unpublished).

[7] A. Bratenahl, University of California Radiation Laboratory Report UCRL-1842 (unpublished); Phys. Rev. **92**, 538(A) (1953).

[8] J. M. Teem and U. E. Kruse, Phys. Rev. **95**, 664(A) (1954).

unit integrated beam at the deuteron laboratory scattering angle Θ; N, the number of target deuterons per cm^2 measured in the direction of the beam; n, the number of beam protons per unit integrated beam, and Ω, the solid angle subtended at the target by the defining counter. The laboratory differential cross section is then

$$\sigma(\Theta)=D(\Theta)/Nn\Omega. \quad (1)$$

The heart of the experimental problem is the method of detecting the events. A commonly used detection system for a scattering process involving two charged particles comprises (a) a "defining" counter, which determines the scattering angle under study and the solid angle accepted, (b) a "conjugate" counter, the angular position of which depends upon the kinematics of the process and the solid angle of which must be sufficient to include all partners of particles striking the defining counter, and (c) coincidence and scaling circuits. At the energy used here, however, this system, though effective in reducing general background and in aiding in identification of the process, is insufficient by itself to separate elastic p-d events from those inelastic ones in which the deuteron in the target is broken apart and two fast protons and a neutron emerge.

Inelastic events are troublesome because the angle between the two emergent protons is distributed over a broad range of values that includes the angle characteristic of the elastic events. The broadness arises from the internal motion of the deuteron, as may be seen from an impulse treatment of the kinematics of the inelastic process (see Appendix). An oversimplified picture is that of the beam proton incident upon a moving target proton. Furthermore the ratio of inelastic to elastic cross sections, though dependent on Θ, is always large, being of the order of ten at some angles. Consequently it is kinematically possible for inelastic events to produce coincidences in counters set at the proper angles for observing elastic scattering; moreover, a non-negligible fraction of the total number of events recorded at such angles will be inelastic ones.

Satisfactory separation of the two types of events can be achieved by a detection system which (in addition to detecting both emergent particles in coincidence) identifies the scattered deuterons as deuterons. This can be done by measuring two or more parameters of the particle, such as specific ionization, energy, range, momentum, etc. Each combination of parameters has advantages and disadvantages; for this experiment, specific ionization and energy were chosen. This system affords adequate separation of protons and deuterons, and the equipment necessary is light-weight and physically compact. The principal practical difficulties in its application arise from the requirement that the stopping power of the counter telescope used must be adjusted to the range of the deuteron to be detected; for very small and very large deuteron ranges the method ceases to be feasible.

In the system employed, the specific ionization is approximately measured by the pulse height produced in a counter that is thin compared to the range of the deuteron, and the total energy by the pulse height from a counter thick enough to stop the particle. These pulse heights are displayed on an oscilloscope screen and photographed.

III. APPARATUS

Figure 1 shows a schematic top view of the apparatus located in the bombardment area and a simplified block diagram of the electronic circuits. The source of the 340-Mev protons was the scattered external proton beam of the 184-inch Berkeley cyclotron. Beam extraction, collimation, and integration (the latter done with ionization chamber, condenser, and electrometer) were accomplished in essentially the same way with virtually the same equipment as that used by Chamberlain, Segrè, and Wiegand[9] in their p-p scattering experiments. The targets employed were several pairs of deutero-polyethylene $[(CD_2)_n]$ and carbon disks, the carbon targets being of thicknesses giving in most cases nearly the same number of carbon atoms per cm^2, and

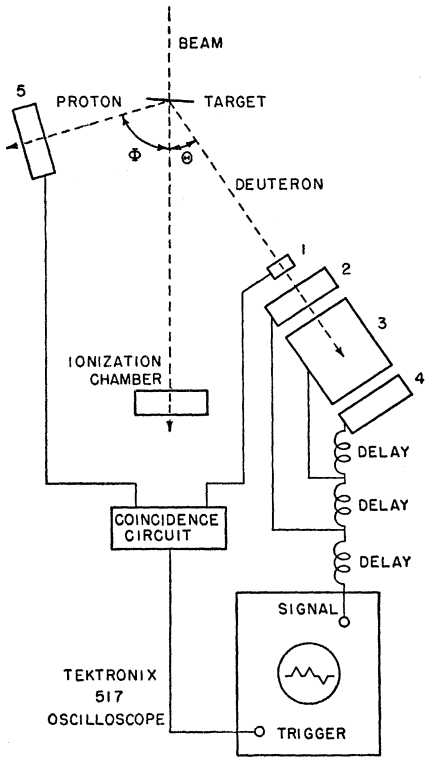

FIG. 1. Schematic top view of apparatus in bombardment area with simplified block diagram of electronic circuits. Telescope I of text depicted. Counters are: 1, defining; 2, specific ionization; 3, energy; 4, "pass-through"; 5, conjugate. Further details in text.

[9] Chamberlain, Segrè, and Wiegand, Phys. Rev. **83**, 923 (1951).

in the others about the same stopping power, as the corresponding CD_2 targets. A typical CD_2 target was 0.13 g/cm² thick.

A. Counters

The deuteron counter-telescope had four different forms, dependent upon deuteron range. Telescope I, used for most angles (70° through 150° center-of-mass angles; deuteron ranges greater than 7 g/cm² of copper), consisted of four scintillation counters, which in the order seen by an incident particle were: a defining counter furnishing a signal for the coincidence circuit, a thin counter ("*dE/dx* counter") to measure the specific ionization, a thick counter ("energy counter") to measure the total energy, and a "pass-through" counter to give a signal when an energetic background particle did not stop in the energy counter. This last was included to aid in the reading of the film, as a major portion of the background protons were of large range compared to the elastic deuterons. Telescope II, for 40° and 50° (c.m. system) (1.2 and 2.5 g/cm² range), consisted of three scintillation counters: one serving the double function of defining and *dE/dx* counter, one to measure the energy, and one as a pass-through counter. The first counter employed stilbene as the scintillator; as it was very thin, the light output was small, and the pulse-height resolution poor, making somewhat uncertain the separation of protons and deuterons. For comparison, Telescope III, being identical to II except for the substitution of a NaI crystal in place of the stilbene, was later employed at 40° and 50°. Telescope IV, used at 30° (c.m. system) (0.45 g/cm² range), consisted of only one plastic scintillation counter; here separation of elastic and inelastic effects was carried out by other than *dE/dx* and *E* identification, which for several reasons—principally the short range—was not feasible. The method of separation is described below in the section on experimental procedure.

For some angles aluminum absorber was added to the telescopes to decrease the range of the incident deuteron. An aluminum absorber wedge was also used to bring the deuterons, whose energy varied with angle across the face of the defining counter, to approximately the same energy before entering the pulse-height counters. The wedge and absorber were placed between counters No. 1 and No. 2 in Telescope I, and in front of the entire telescope in Telescopes II and III.

The areas of the counter faces were chosen so that only a negligible fraction of the deuterons entering the defining counter would be scattered out of the energy counter by multiple Coulomb scattering before stopping, even when the maximum amount of absorber was present. The *dE/dx*-counter thickness was chosen so that (a) the range bite was not so large as to make the energy loss unrepresentative of the specific ionization (and thus spoil the separation of deuterons from protons), and (b) the energy loss was not so small that

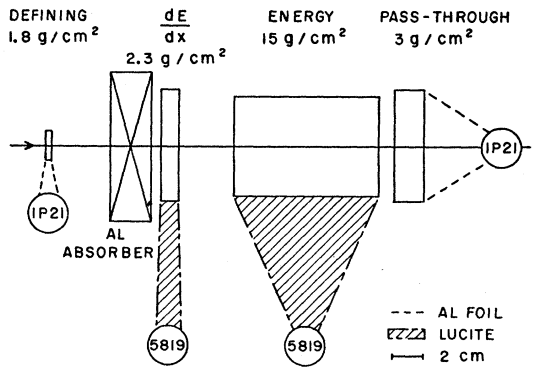

FIG. 2. Schematic diagram of Telescope I. Scintillator dimensions and intercounter spacings approximately to scale. All counters when viewed end-on were square, except pass-through counter, which was circular. Thicknesses in g/cm² copper equivalent.

the Landau effect and statistical fluctuations in the number of photoelectrons released from the photocathode would decrease the pulse-height resolution of the counter to a point that would mask the separation. Ideally the energy counter should have sufficient depth to stop the desired deuterons. However, the maximum deuteron range encountered in the experiment was 44.7 g/cm² of copper, and it was not thought practical to construct a counter with good pulse-height resolution with that large a stopping power. Consequently, the energy counter in Telescope I was only 15 g/cm² copper equivalent in depth.

Figure 2, which is a schematic drawing of Telescope I, indicates the general nature of the counters employed; the scintillator dimensions and intercounter spacings are drawn approximately to scale. The phosphor used in all counters, except those which have been otherwise described, was a liquid one developed by Kallmann[10]: 0.3% *p*-terphenyl and 0.001% diphenylhexatriene (by weight) dissolved in phenylcyclohexane.

Accurate pulse-height distribution curves for monochromatic particles incident on the counters were not taken for all counters. However, it may be stated that under the operating conditions encountered, the pulse-height counters had distributions of about 15% full width at half maximum, except for the stilbene and the plastic counters, which had about 25%.

For the other coincidence counter, designated as the conjugate counter or proton counter, at different times either a stilbene or a liquid-phosphor counter was used. All photomultiplier tubes were magnetically shielded.

B. Electronic and Photographic Apparatus

Figure 1 depicts a simplified block diagram of the electronic circuits. Omitted from the figure are: (a) a second coincidence circuit fed by signals from the defining and conjugate counters but with one input delayed with respect to the other by 6×10^{-8} sec (by a

[10] H. Kallmann and M. Furst, Phys. Rev. **81**, 853 (1951).

length of coaxial cable) so that the output furnished a continuous monitor of the accidental coincidence rate[11]; (b) distributed amplifiers that were necessary at several points; and (c) scalers reading the outputs of both coincidence circuits, the number of sweeps triggered on the Tektronix model 517 oscilloscope, and the individual counting rates in the coincidence counters.

The coincidence circuits employed were at different times a germanium diode circuit or a circuit essentially that of Garwin.[12] The effective resolving time of either circuit, which was limited by the width of the input pulses, was about 2×10^{-8} sec.

The sweep of the oscilloscope was triggered by either the direct or delayed coincidence output as desired, and the number of sweeps was monitored by a scaler connected to the "gate output." It was found impossible to adjust the trigger amplifier control so that the number of sweeps exactly equaled the number appearing on the coincidence scaler. However, the deuteron counting rate as seen on the film was found to be insensitive within statistics even to rather large discrepancies in the two readings. This merely implies that the deuterons were well on the counting plateau.

The signals from the pulse-height counters were taken from the anode or last dynode of the phototubes (depending upon the sign of pulse desired), suitably delayed with respect to one another to separate them on the oscilloscope trace, and fed to the signal input of the oscilloscope through a common delay which controlled their position on the sweep. Regulated power supplies were used throughout the pulse-height circuits, and the stability as checked by a pulse generator was excellent.

A brass hood coupled the oscilloscope face to a General Radio 35-mm oscilloscope camera, in which the film was moved continuously at an adjustable rate of about 1 foot per minute. The aperture used was $f/1.5$. Easily developable traces were produced on Eastman Linagraph Pan film even at writing speeds of 200 cm per microsecond. The film was developed either in Eastman D-19 or concentrated Atkinson A-72 developer.

IV. EXPERIMENTAL PROCEDURE

A. Procedure for Taking Data

For each day's run, following alignment of the apparatus with the beam, the counters were set to observe *p-p* scattering from a CH_2 target, and a series of adjustments and tests of the electronic gear was carried out. Among these were the following. The coincidence rate due to hydrogen was observed as a function of the relative delay of one coincidence input with respect to the other (for both direct and delayed outputs) to check timing. The direct coincidence rate was further observed to obtain counting plateaus with respect to phototube voltages by varying the voltage on each coincidence counter in turn. The beam intensity was then varied, and the coincidences per unit integrated beam ("integrator volt," or "I.V.") were plotted *vs* beam intensity. This test revealed whether there was any systematic difference between the delayed coincidence rate and the actual accidental rate. The last adjustment made using the CH_2 target and *p-p* scattering was to observe on the oscilloscope the pulses produced in the pulse-height counters by these protons of known (calculated) energy, and to set the gains of amplifiers in the pulse-height system so that the pulses from deuterons to be recorded later in the day would be neither too small to be accurately read nor large enough to saturate any amplifier. A few of these *p-p* scattering pulses were recorded on film to furnish energy-loss calibration points. To determine the beam energy a "Bragg curve" was taken—the ratio of readings from two thin ionization chambers placed in the beam *vs* the amount of copper absorber inserted between the chambers.

When these preliminary operations had been accomplished, the CD_2 and associated carbon targets were put into place, the counters set at the desired angles and distances from the target, and elastic *p-d* scattering data recorded. For each angle film was exposed for each of the three targets (CD_2, carbon, and no target, or "blank") with triggering of the oscilloscope at different times from the direct and the delayed coincidence outputs—six arrangements in all. The bulk of running time was spent on CD_2 and carbon targets with direct triggering.

Intermittent checks on the gain stability of the pulse-height system were made with a pulse generator or by reverting to a short run of *p-p* scattering. Two alterations were made in counter geometry to aid in establishing that the effect, the whole effect, and nothing but the effect was being measured. One consisted in increasing the solid angle subtended by the conjugate counter to check the adequacy of the solid angle normally employed, which was calculated for each scattering angle from simple geometrical considerations of beam diameter, defining-counter size and position, angular settings of counters, target angle to beam, and (to allow for multiple scattering) target thickness and proton and deuteron energies. Because of low counting rates and consequent large statistical errors, this test was not conclusive. Nevertheless, because the formulas used in calculating the solid angle were based on similar formulas used in previous work by Chamberlain and Stern, and by Chamberlain, Segrè, and Wiegand, and because a liberal safety margin was allowed, we do not believe that more than a few percent of the proton partners to elastic deuterons striking the defining counter were not counted. The second alteration in geometry was to verify that the deuteron counting rate was peaked at the included angle for elastic events,

[11] The fine structure of the proton beam determines the delay necessary. The particles emerge in bursts of about 0.5×10^{-8} sec in duration with peaks separated by 6×10^{-8} sec.

[12] R. L. Garwin, Rev. Sci. Instr. 24, 618 (1953).

as calculated from relativistic kinematics, and zero to either side. Figure 3 shows the deuteron counts per integrator volt as a function of the angular setting of the proton counter. The peak is seen to exist and to be at the expected angle. A further identification of the elastic process was obtained by comparison of the calculated and observed deuteron energies, the latter as shown by the pulse heights.

B. Procedure in Reading Film

The developed film was read on a microfilm viewer, on the screen of which was superimposed a lucite grid with rulings every two mm. Typical pulse heights on the viewer were 10 to 60 mm high, and could be read to 1 mm. Figure 4 shows a typical section of film from Telescope I. A single high-energy proton or deuteron produced a pattern of two pulses (or three, if it had been energetic enough to pass through the energy counter); the relative spacings of the pulses were determined by the artificial delays introduced for that purpose. When spurious pulses due to other particles were present on the sweep (as in the next-to-lowest sweep in the figure) the spacings and position of the pattern indicated which pulses should be read.

The heights of the pulses from the dE/dx and energy counters were tabulated for each pattern (and the presence or absence of the pulse from the pass-through counter was recorded). The pair of numbers was plotted as a point on graph paper with dE/dx pulse height as ordinate and energy pulse height as abscissa. Patterns without a pass-through pulse were plotted as dots, and those with one as crosses. Figure 5 shows typical results (for Telescope I) when a little more than one hundred points were plotted: a CD_2 target was in the beam in this case. The general features of the plot are as follows: (a) a band identifiable as the locus of protons, (b) an "island" due to a group of nearly monoenergetic deuterons (from elastic p-d events), (c) a tail consisting almost entirely of points from patterns including a pass-through signal (crosses), and (d) a few widely scattered points.

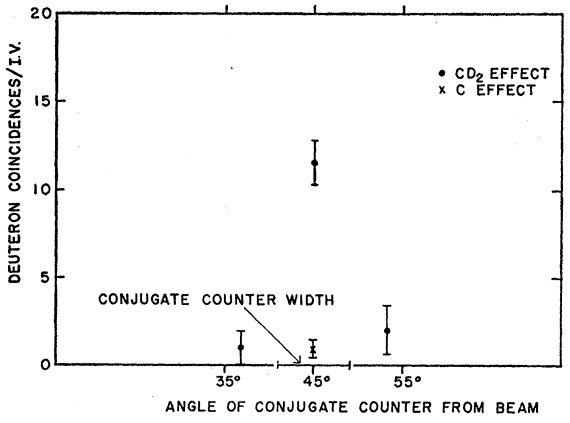

FIG. 3. Elastic peak as shown by the variation of the number of deuterons from CD_2 per integrator volt *versus* angle of proton counter with respect to beam. Deuteron counter was fixed at 54°. Angles in laboratory system.

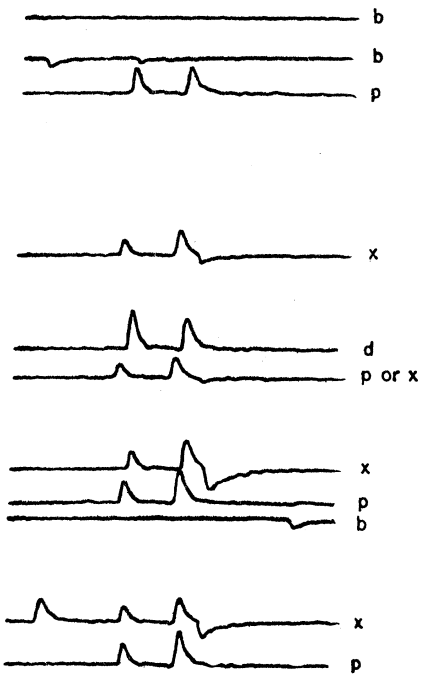

FIG. 4. Typical section of film, showing shape and spacing of pulses: d indicates a deuteron, p a proton, b a blank sweep (no particle) and x a pass-through (a particle not stopped in the energy counter).

The collection of deuterons from p-d events into an island despite the variation of the deuteron energy across the finite width of the defining counter was accomplished by a wedge of aluminum absorber, as mentioned previously.

The tail is due to protons that are too energetic to be stopped in the energy counter; they produce a dE/dx pulse height that is proper for their energy, but a pulse height from the energy counter that is much too low for their energy. A very energetic deuteron of course falls into a similar tail belonging to the deuteron locus. Furthermore, the deuteron and proton tails would coincide in part.

Some of the widely scattered points are due to particles that scatter out of the counters and thus do not lose in the counters the proper amounts of energy, and some probably to the simultaneous passage through the telescope of two scattered particles. The probability of the latter type of event was very small at the counting rates employed; the duration of the pulses was short enough so that only when two or more particles were scattered into the telescope during the same burst (of 0.5×10^{-8} sec duration) would their pulses be superimposed so as to appear as a single pulse. Some of the widely scattered points may be tritons, though none have been positively identified as such.

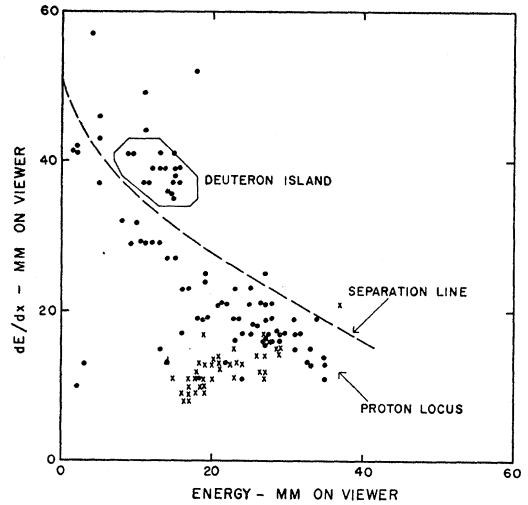

FIG. 5. Typical plot of data from film taken with Telescope I, for 70° center-of-mass scattering. See text for explanation of features of the plot.

Blank sweeps such as in Fig. 4 can be attributed to products of the bombardment having such short range that they cannot reach the pulse-height counters. Typically about 6% of the identifiable particles observed in the telescope were deuterons.

The analysis to separate deuterons from protons was carried out by four different methods: A, for the 70°–110° range of center-of-mass scattering angles, and for 40° and 50° when using Telescope III; B, for 40° and 50° when using Telescope II; C, for 130° and 150°. At 30°, an entirely different procedure was involved and will be discussed separately below.

Method A was employed when the plots were similar to Fig. 5, in which the deuteron island and proton locus are well separated. The procedure was to read all sweeps until the position of the loci became evident, and subsequently to read only those pulse patterns whose dE/dx pulse put them near the island. This saved considerable time, as most particles observed were high-energy protons. The location of the island was checked against an expected position calculated on the basis of the p-p scattering data. It was necessary to choose, on the basis of all sweeps read, the outlines of the island on the graph which would be considered to include all elastic p-d deuterons. While the separation of protons and deuterons was reasonably unambiguous, the presence on the deuteron locus of a few deuterons of varying energies due to the carbon portion of the target made it unreasonable to count all observed deuterons on the locus as coming from elastic p-d scattering. Despite the smallness of the number of deuterons, the grouping was close enough that the outlines of the island could be drawn without much difficulty. Islands of larger sizes were tried, and it was found that the number of deuterons in the added area, after subtraction of carbon counts and accidentals, was zero within statistical error. The outline on Fig. 5 shows the island chosen in one case. (This outline was drawn on the basis of many more points than are shown in the figure.) With the island thus chosen, the number of deuterons for each of the six arrangements of target and triggering was counted.

Method B was employed because the poorer pulse-height resolution in Telescope II made the separation somewhat ambiguous. Let us consider again the method of plotting points on a graph of dE/dx pulse height *versus* energy pulse height. The proton and deuteron loci are approximately parallel curves. If a group of equally spaced curves parallel to the proton curve is drawn in, and the distribution of points in the "channels" thus created is tabulated, the result is an approximate mass spectrum of the particles seen by the telescope. Figure 6 shows, for example, the mass spectrum obtained with a portion of data from Telescope I. The data from Telescope II were treated as follows: first, data from p-p scattering were used to determine the proton locus and draw in the channels; Fig. 7(C) shows the spectrum obtained. CD_2 data were also read and plotted as a mass spectrum using the same channels [Fig. 7(A)]. The proton portion of the latter was then removed by subtracting the proton curve C normalized with suitable weighting to a best fit with the spectrum in channels zero through minus 3 of the CD_2 data. The resulting deuteron spectrum [Fig. 7(B)] was integrated to obtain the number of deuterons. The same treatment was applied to the other arrangements of targets and triggering. Because of the uncertainties involved, the systematic error due to the separation method has been taken larger for method B than for A.

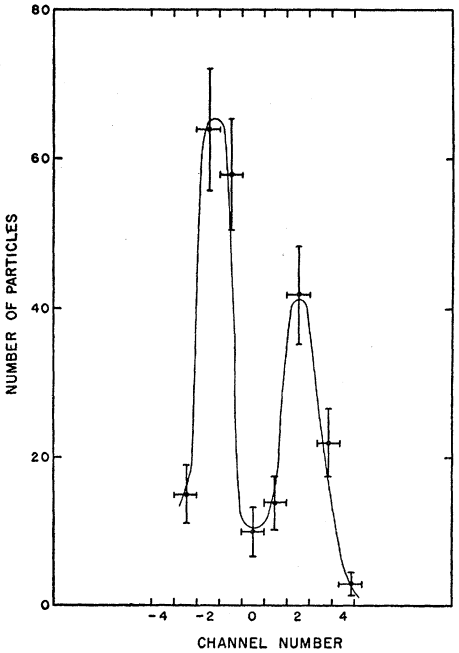

FIG. 6. "Mass spectrum" for a portion of data taken with Telescope I.

Method C was employed for 130° and 150° because for these angles the deuterons to be observed had ranges of 36 and 45 g/cm² copper, respectively. The amount of absorber in the telescope that would be necessary to cause these deuterons to stop in the energy counter was considered excessive. Consequently, only about one inch of aluminum absorber was used; the desired deuterons were thus allowed to fall on the "tail" of the deuteron locus. Because of the partial overlap of the proton and deuteron tails, there was the possibility that some of the inelastic protons could be confused with the deuterons. Hence absorber was placed in front of the proton counter to reduce the amount of observable inelastic scattering, and film data were then taken not only with the proton counter at the proper angle to observe the elastic events, but also at angles to either side, to evaluate the amount of inelastic scattering included. After the initial survey, only sweeps with pass-through pulses needed to be read. Energy calibration and the choice of deuteron island were carried out similarly to the same steps in method A. The number of points found in the island when the proton counter was set at other angles than the elastic angle was found to be zero within statistics after the subtraction of contributions due to accidentals and carbon. We therefore felt justified in considering that all the apparent deuterons at the elastic angle were indeed deuterons, and the statistical counting errors were computed on that basis. However, the systematic error in the separation of protons and deuterons has been taken somewhat larger for these angles than for method A.

For the 30° measurement (method D), Telescope IV, consisting of only one counter, was employed. Because of the short deuteron range (0.45 g/cm² copper) the dE/dx-and-E method was not feasible. Instead, use of a thin target and a defining counter of small angular aperture as the proton counter made the desired conjugate deuterons nearly monoenergetic; the deuteron counter stopping power was chosen so that these deuterons would just be stopped in the counter. Their pulse heights were then larger than those produced by protons of any velocity. Satisfactory application of this detection system was aided by the large elastic cross section, and the relatively small ratio of inelastic to elastic cross sections, at this angle. Pulses from this single counter were photographed under p-p scattering conditions as well as with the other targets. A plot of the number of pulses in each pulse-height interval *vs* pulse height showed for CD_2 a peak at the high end attributable to deuterons. Film was taken with several different thicknesses of thin absorber preceding the counter to test the method; data taken with the arrangement that gave the best separated peak were those used in computing the cross section. However, the systematic error assigned to this separation method was taken larger than that for the dE/dx-and-E approach.

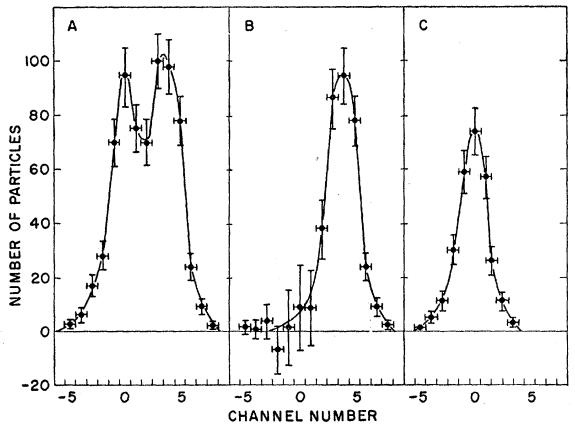

FIG. 7. "Mass spectra" for a portion of 40° center-of-mass data taken with Telescope II. (A) With CD_2 target, showing both protons and deuterons. (B) Same, but with protons subtracted by method explained in text. (C) Proton spectrum used in subtraction (from p-p scattering).

V. REDUCTION OF DATA

A. Subtraction of Effects Due to Carbon and Accidental Coincidences

It had been initially expected that the number of deuterons from the carbon in the polyethylene would be very small, since the cross section expected for pickup[13] at 340-Mev bombarding energy is very low, and especially since the detecting apparatus used required a coincidence of the deuteron with a charged particle at an angle with respect to the deuteron that was characteristic of p-d scattering (94° to 137° lab in this experiment). However, such deuterons were found in non-negligible quantities. Two mechanisms were considered possible for this effect. One was that the beam proton is able to knock a complete deuteron out of the carbon nucleus. The second, thought more likely, was that a nucleon-nucleon collision takes place inside the carbon nucleus, and that the recoil or deflected particle in emerging from the nucleus picks up a partner at the surface to form a deuteron. The pick-up probability for the incident proton would be enhanced by the reduction in momentum following collision. The angle between the proton and deuteron for this process would vary, but perhaps be peaked near 90°.

In this experiment, however, the deuterons from carbon were treated only as background, and no attempt was made to study them further. It was subsequently learned that the second process is the topic of a theoretical paper by Bransden.[14] This "indirect pickup" by both protons and neutrons has since been studied experimentally in detail by Hess[15]; his results confirm its existence.

[13] G. F. Chew and M. L. Goldberger, Phys. Rev. **77**, 470 (1950) and J. Hadley and H. York, Phys. Rev. **80**, 345 (1950).
[14] B. H. Bransden, Proc. Phys. Soc. (London) **65**, 738 (1952).
[15] W. N. Hess, University of California Radiation Laboratory Report UCRL-2670 (unpublished).

Rather involved algebraic expressions have been derived to make an accurate subtraction of backgrounds. Since most of the terms in the final expression are extremely small in most cases, we restrict our attention here to the following simpler form that is usually accurate to a few percent, namely,

$$D=CD_2-RC-(1-R)Bl, \quad (2)$$

where D is the number of deuterons counted per unit integrated beam due to deuterium in the target, CD_2 is the number of deuterons counted per unit integrated beam from a CD_2 target (and restricting the count to those that fall within the "deuteron island" of Fig. 5), C and Bl are analogously defined for the carbon target and blank (no target), and R is the ratio of carbon surface density in the CD_2 target to carbon surface density in the carbon target. The delayed coincidence counts do not appear in the above expression, but were useful in evaluating small correction terms that are not presented here.

B. Corrections for Attenuation in Absorbers and Counters

Corrections to the observed data had to be made because of deuteron attenuation by inelastic scattering and by stripping, both of which could take place in the absorbers and in the counters themselves. For attenuation of the elastic protons due to the absorber employed in some cases to precede the conjugate counter, the cross sections measured by Kirschbaum[16] were used.

For attenuation of the deuterons, a total cross section for all processes except diffraction scattering for deuterons of an average energy of about 140 Mev was available.[17] As data for other deuteron energies were not available, and as it is believed that the attenuation cross section is not strongly dependent on energy, the value for 140 Mev was used throughout. An error of 10% was assigned to the cross section employed.

In the calculation for deuteron attenuation, all counters preceding the energy counter were treated as absorbers, because any processes deflecting or breaking up the deuteron in these counters would cause the deuteron either to be lost completely or to give a pulse-height pattern not characteristic of a deuteron. In the energy counter, however, a few stripping events would not cause a reduction of the energy pulse height large enough to make the deuteron have a pulse-height pattern not in the deuteron island. The number of the latter type of event was estimated, and the error in the estimate was assumed to be 50%.

Table I in the next section shows (along with the experimental results) the correction factor for attenuation that was applied at each angle.

[16] A. J. Kirschbaum, University of California Radiation Laboratory Report UCRL-1967 (unpublished).

[17] Millburn, Birnbaum, Crandall, and Schecter, Phys. Rev. **95**, 1268 (1954).

C. Target

The target material was analyzed chemically and found to have a ratio of total hydrogen to carbon content of 1.97 ± 0.02 (numbers of atoms). Further analysis by mass spectrometry showed the deuterium fraction (by number) of the hydrogen content to be $(94\pm1)\%$. Both analyses were carried out by Dr. Amos Newton of this laboratory.

A very thin foil of the target material was also analyzed by infrared absorption techniques. This analysis, which was done by Professor George Pimentel of the University of California Chemistry Department, gave values from 5% to 7% for the H^1 fraction.

A value of $(94\pm1)\%$ was therefore used in the calculations, and the number of carbon atoms was taken as one-half the number of H^1 plus H^2 atoms.

D. Sample Calculation

We give as an example the calculation of the first case of 110° scattering listed in Table I.

Targets.—The CD_2 target was 0.1312 g/cm^2 thick, and therefore contained 0.941×10^{22} deuterons per cm^2 and 0.497×10^{22} carbon atoms per cm^2. The CD_2 target was oriented with its normal 11.2° from the beam, so the surface density of deuterons in the beam direction was $N=0.959\times10^{22}$, and of carbon atoms was 0.507×10^{22}. The carbon target was at 12° to the beam, with 0.530×10^{22} carbon atoms per cm^2 in the beam direction.

Beam current.—One volt on the recording millivoltmeter (one "integrator volt") indicated $C/q\mu$ protons in the beam, where C was the capacity employed (0.985×10^{-6} farad), q the elementary electronic charge (1.602×10^{-19} coulomb), and μ the "multiplication factor" of the ion chamber. This multiplication factor (not related to gas multiplication as in proportional counters) is the result of the formation of a large number of ion pairs by each proton passing through the chamber, and may be defined as the ratio of the charge received by the ionization chamber from the passage of a single proton to the charge carried by the proton.

Calibration against a Faraday cup had shown that we have $\mu=1040$ for 340-Mev protons in an ionization chamber of effective depth of 2 inches filled with argon to 100 cm Hg absolute pressure at 20°C. The chamber employed in taking the data under discussion had a depth of 2.028 inches, and was filled to 82.5 cm Hg at 21.0°C. Therefore, $\mu=867.4$. Hence one integrator volt was equivalent to

$$n=0.985\times10^{-6}/[(1.602\times10^{-19})(867.4)]$$
$$=0.709\times10^{10} \text{ protons.}$$

Solid angle.—The face of the defining counter was 2.00×2.05 cm, and the counter was 80.2 cm from the target position. The solid angle subtended was therefore $\Omega=6.38\times10^{-4}$ steradian.

Number of events observed.—From analysis of the films,

we had the following numbers of events and their associated statistical errors:

$CD_2 = 49 \pm 7$ in 10.224 I.V., or 4.79 ± 0.69 per I.V.,

$C = 1 \pm 1$ in 3.074 I.V., or 0.325 ± 0.325 per I.V.,

$Bl = 0 \pm 1$ in 0.509 I.V., or 0 ± 1.96 per I.V.

Therefore, from Eq. (2), the number of elastic p-d events per integrator volt was $D = 4.48 \pm 0.762$, where the ratio R of the number of carbon atoms per cm^2 in the CD_2 target to that in the carbon target was 0.957.

Cross section.—Therefore the laboratory cross section, uncorrected for attenuation, was

$$\sigma(\Theta)_{\text{lab}} = D/nN\Omega = 0.103 \pm 0.018 \text{ mb/steradian.}$$

To convert to the center-of-mass system, $d\cos\Theta_{\text{lab}}/d\cos\theta_{\text{c.m.}} = 0.293$, giving $\sigma(\theta)_{\text{c.m.}} = 0.0303 \pm 0.0053$ mb/steradian.

Attenuation correction.—No absorber was present in front of the proton counter. For that in front of the deuteron telescope, and for the telescope counters themselves, we used $I/I_0 = \exp(-\rho\sigma x)$, where I_0 = the number of elastically scattered deuterons actually incident on the telescope, I = the observed number of deuterons, ρ = numerical density of nuclei, σ = attenuation cross section per nucleus, and x = thickness of absorbing material in cm. The resulting correction factor was 1.59 ± 0.12, and the final value for the cross section was therefore 0.0482 mb/steradian with 17% standard deviation counting error, as listed in Table I.

E. Discussion of Errors

The following is a listing of the known sources of systematic error and the estimates of the sizes of the errors. These errors are treated as standard deviations and combined by taking the square root of the sum of squares.

Geometry.—The calibration of the angles of the scattering table was accurate to about 0.5°, and the alignment of the table with respect to the beam accurate to 1°. These errors result in a 5% uncertainty in the cross sections at angles 30° through 70° and at 150°, but result in negligible uncertainty at other angles, where the cross section is slowly varying. The distance from target to defining counter was considered known to 1%, so a resulting 2% error in solid angle was included. Furthermore, there was estimated to be a 1% error in the actual area of the defining counter, and a 3% error due to edge effects in the defining counter. Possible loss of counts resulting from insufficient solid angle of the conjugate counter has been assigned a 3% error.

Beam current.—A 2% error was attributed to the absolute calibration of the ionization chamber (determination of the multiplication factor), and a 1% error to possible lack of complete saturation in the ionization chamber. The condenser in the electrometer circuit was calibrated to 0.3%, and the voltage reading of the electrometer to 1%.

Targets.—The ratio of carbon to hydrogen content of the polyethylene targets was known to 2%, and the fraction of deuterium in the total hydrogen known to 1%. The surface densities of the polyethylene targets were known to 2%. The orientation angle of the target with respect to the beam was in every case determined to 2 degrees. This resulted in an error in cross section of 5% at 30° and 130°, 6% at 150°, and somewhat smaller errors at other angles of scattering.

Background subtraction.—Errors in the subtraction of counting rates due to carbon and due to accidental coincidences were estimated to give rise to 3% uncertainties in the cross sections.

Counter-telescope efficiency.—The errors in cross sections from losses due to multiple Coulomb scattering and diffraction scattering were estimated to be 3%. An increase in the number of apparent deuterons due to simultaneous passage of two particles through the counter telescope could give rise to a 2% error. The increase in the number of deuterons due to pickup inside the absorber or the counter telescope by protons incident on the telescope was negligible.

Counting of deuterons.—Errors resulting from inadequate separation of protons from deuterons or from the manner of choice of the deuteron island have been assumed to contribute 5% for method A, 15% for method B, 10% for method C, and 15% for method D.

Attenuation corrections.—The computations of nuclear attenuation in the absorbers used contributed errors ranging from 0 to 8%; these errors are listed separately in Table I.

Variation in beam energy.—Unrecognized variations in the beam energy could account for errors estimated at 4%, since the cross sections change fairly rapidly with energy.

Possible polarization of the beam.—Recent studies[18] have shown that the beam as used in this experiment was unpolarized, so no error has been included for this effect.

VI. EXPERIMENTAL RESULTS

Table I shows the experimental results obtained. For each center-of-mass scattering angle θ studied, the following quantities are tabulated: (1) corrected center-of-mass differential cross section in millibarns per steradian; (2) absorber correction factor employed; (3) statistical error (standard deviation); (4) error in absorber correction; (5) error in counting deuterons in the film analysis (separation of protons from deuterons and choice of deuteron island); (6) combined systematic error from other sources; and (7) total error, combined from all sources. Measurements taken under different experimental conditions are shown on separate lines. Averages are weighted averages.

[18] Chamberlain, Segrè, Tripp, Wiegand, and Ypsilantis, Phys. Rev. **93**, 1430 (1954).

TABLE I. Experimental results and errors. The cross sections and angles are in the center-of-mass system. The cross sections have been corrected for attenuation. In the center-of-mass system, angles are known to 2°, and the resolution is 0.9° for 30°, 5.7° for 40° and 50° (first row), 2.9° for 40° and 50° (second row), and 2.8° for the other angles.

θ deg.	$\sigma(\theta)$ mb/sterad	Attenuation correction factor	Statistical error (s.d.) (%)	Error in att'n. corr. (%)	Error in separation (%)	Other syst. errors (%)	Total error (%)
30	2.22	1.00	15	0	15	11	24
40	1.04	1.05	8	1.7	15	10	
	0.829	1.05	9	1.7	10	10	
	0.892 (av)	...	...	...	...	...	15
50	0.392	1.07	11	1.9	15	10	
	0.389	1.05	10	1.9	10	10	
	0.390 (av)	...	...	...	...	...	15
70	0.104	1.11	32	1.6	5	9	
	0.109	1.11	13	1.6	5	9	
	0.108 (av)	...	...	...	...	...	16
90	0.0402	1.28	18	6.2	5	8	
	0.0581	1.28	23	6.2	5	8	
	0.0468 (av)	...	...	...	...	...	16
110	0.0482	1.59	17	7.6	5	8	
	0.0399	1.57	13	7.9	5	8	
	0.0424 (av)	...	...	...	...	...	16
130	0.0440	1.50	20	7.7	10	9	
	0.0567	1.43	30	7.3	10	9	
	0.0467 (av)	...	...	...	...	...	23
150	0.101	1.46	11	7.5	10	11	
	0.0914	1.43	21	7.3	10	11	
	0.0986 (av)	...	...	...	...	...	20

In Fig. 8, the averaged differential cross section in the center-of-mass system is plotted on a logarithmic scale *versus* center-of-mass scattering angle along with data of other workers at lower energies. The total error is shown, and the solid lines have been drawn only to guide the eye.

Although only approximately half the total cross section is included in the measured range of 30° to 150°, the differential cross section for angles less than 30° was not measured because the deuteron energy becomes too low to permit good identification of the deuteron, and at angles greater than 150° the proton energy becomes too low for satisfactory use of the coincidence method. It is nevertheless worth while to estimate the total cross section; that part under the measured curve integrates to 2.9 millibarns. The measured curve can be extrapolated below 30° and above 150°; if this is done by assuming $\sigma(\theta)$ to be constant at 2.22 and 0.0986 mb/steradian, respectively, the total becomes 4.25 mb, which is certainly a lower limit. If the cross section is extrapolated by eye, using lower energy results as a guide, the total obtained is 5.97 mb, to which we assign a 20% error. This may be compared with the sum of the free *p-p* and *n-p* cross sections, i.e., 24 plus 33, or 57 millibarns.

VII. INTERPRETATION

The problem of high-energy nucleon-deuteron scattering has been considered theoretically by several authors.[19] We shall confine ourselves to a nonrelativistic treatment, and discuss the interpretation of our experimental results from the viewpoint of the impulse approximation,[20] which allows us to relate the *p-d* scattering to *p-p* and *n-p* scattering parameters.

We can picture the elastic scattering of protons by deuterons in terms of the superposition of two-body scattering amplitudes (*p-p* and *p-n* scattering amplitudes) provided that the following conditions can be met. Firstly, the collision process must occur rapidly enough so that the deuteron binding forces would not, in the time of collision, make an appreciable alteration in the state of the deuteron. Secondly, the amplitude at one nucleon of the deuteron due to scattering by the other nucleon should be small compared to the amplitude of the incident wave, in order that the amount of double scattering be small. Both these conditions can be satisfied fairly well, providing the separation of particles in the deuteron is reasonably large.

There is some correlation between the angle of scattering and the separation of particles in the deuteron, so the conditions mentioned in the previous paragraph may be met at small angles of scattering, and not at larger angles. The correlation arises from the fact that in large-angle scattering, with the associated large momentum transfer to the deuteron, one must be concerned primarily with the high-momentum components of the deuteron ground-state wave function, which are predominantly associated with small separation r between the nucleons of the deuteron.

Chew gives the basic impulse approximation result for this problem in a form sufficiently general (at least in Born approximation) to include all types of nuclear forces:

$$\frac{d\sigma_{pd}}{dK^2}=\frac{16}{9}S(K)\{|r_{np}{}^0+r_{pp}{}^0|^2+\tfrac{2}{3}|\mathbf{r}_{np}'+\mathbf{r}_{pp}'|^2\}, \quad (3)$$

where $K=2k\sin(\theta/2)$ is the momentum transfer to the deuteron in wave-number units, k is the incident wave number, and θ the scattering angle, all in the center-of-mass system. $S(K)$ [or $S(\theta)$] is the form factor or sticking factor for the deuteron and is found from

$$S^{\frac{1}{2}}=\int\psi_0{}^2(r)\exp(i\mathbf{K}\cdot\mathbf{r}/2)d\mathbf{r},$$

in which $\psi_0(r)$ is the ground-state deuteron wave

[19] G. F. Chew, Phys. Rev. **74**, 809 (1948); **80**, 196 (1950); **84**, 710 (1951), **84**, 1057 (1951); T. Wu and J. Ashkin, Phys. Rev. **73**, 896 (1948); R. L. Gluckstern and H. A. Bethe, Phys. Rev. **81**, 761 (1951); B. H. Bransden, Proc. Roy. Soc. (London) **A209**, 380 (1951); Horie, Tamura, and Yoshida, Progr. Theor. Phys. (Japan) **8**, 341 (1952); P. B. Daitch and J. B. French, Phys. Rev. **85**, 695 (1952); reference 2.

[20] G. F. Chew and G. C. Wick, Phys. Rev. **85**, 636 (1952) and papers of Chew listed in footnote 19.

function. The r^0 and $\mathbf{r}'$ are two-body scattering amplitudes (designated as nonspin-flip and spin-flip amplitudes respectively) and are normalized by

$$\frac{d\sigma}{dK^2}=|r^0|^2+|\mathbf{r}'|^2$$

for nucleon-nucleon scattering. Equation (3) does not include double-scattering effects.

There are three aspects of Eq. (3) that might conceivably be tested by experiment: (a) comparison with experiment of a purely theoretical prediction of the p-d scattering utilizing two-body amplitudes calculated from reasonable nucleon-nucleon potentials; (b) comparison with experiment of a prediction utilizing two-body amplitudes derived experimentally; and (c) comparison of $S(K)$ as revealed by experiment with S calculated for various assumptions for the form of $\psi_0(r)$.

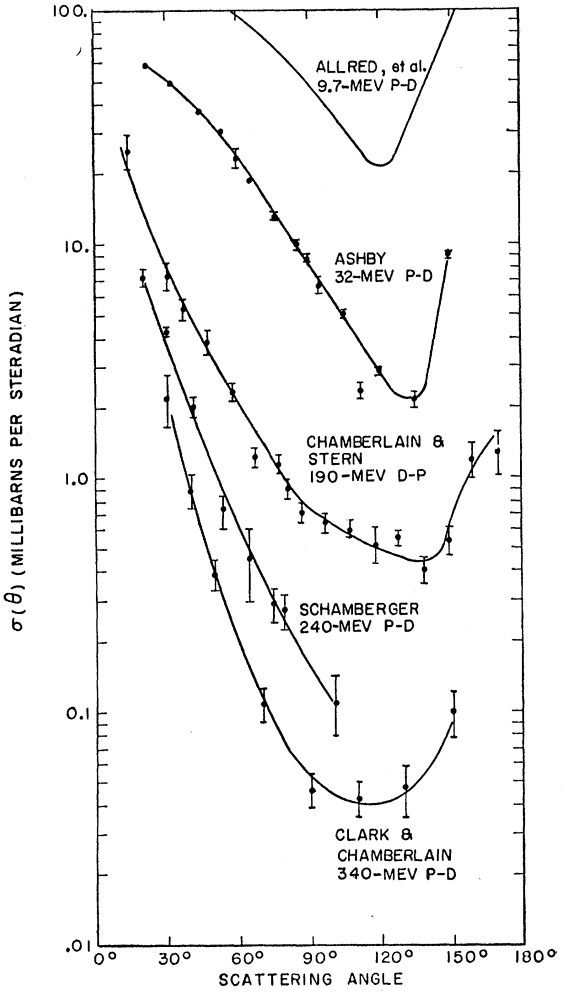

FIG. 8. Comparison of our experimental results with experimental data of other workers at lower energies. Both coordinates in center-of-mass units. Total (statistical and systematic) errors shown. Solid lines are only to guide the eye.

Alternative (a) is a program of larger magnitude than we wish to undertake at this time. Alternative (b) is beset by the difficulty that the experimental n-p and p-p cross sections do not give without some theoretical assumptions the separate r^0 and $\mathbf{r}'$ that we desire nor their relative phases. The polarization experiments currently in progress[21] give additional parameters[22] to aid the separation but still leave ambiguities resolvable only by further experiments. Alternative (c) possesses real merit only if the r^0 and $\mathbf{r}'$ are known experimentally; however, we may easily calculate $S(K)$ for a variety of n-p potentials to see at what values of K reasonable potentials yield significantly different values of S.

It is convenient to follow the analysis of Chamberlain and Stern and define the quantity Δ through the relation

$$\sigma_{pd}(\theta)=(16/9)S(\theta)\{\sigma_{np}(\theta')+\sigma_{pp}(\theta')\}\Delta, \qquad (4)$$

where $\sigma_{np}(\theta')$ and $\sigma_{pp}(\theta')$ are the experimental result for the center-of-mass nucleon-nucleon differential scattering at angles θ' and laboratory bombarding energies T_0' related[2,23] to the p-d center-of-mass angle θ and laboratory energy T_0 by

$$\begin{aligned} T_0'&=T_0(25-7\cos\theta)/18;\\ \cos\theta'&=(-7+25\cos\theta)/(25-7\cos\theta). \end{aligned} \qquad (5)$$

We have Δ equal to 1 if there is no interference between n-p and p-p scattering, greater than 1 for constructive interference, and less than 1 for destructive interference. The quantity Δ is observed experimentally to vary from about 1 at small scattering angles to about 0.5 at 80° in 190-Mev d-p scattering.[2] The fact that Δ is of this order indicates that interference effects in the p-d case are not large. The present stage of experiment and theory thus allows us the comparison of various calculated values of $S(K)$ with $S(K)\Delta$, which from Eq. (4) is equal to $(9/16)\sigma_{pd}/(\sigma_{np}+\sigma_{pp})$.

We have calculated $S(K)$ for three different potentials: (a) a Hulthén potential, (b) a Hulthén potential displaced from the origin by a hard core, and (c) a square well, each with parameters adjusted to fit the experimental values of the deuteron binding energy and the triplet effective range. For (a) the potential is $Ve^{-\xi r}/(1-e^{-\xi r})$ with $V=-76.91$ Mev and $\xi=1.1496\times10^{13}$ cm^{-1}; for (b) the hard-core radius is taken as $b=0.6\times10^{-13}$ cm in accord with Jastrow,[24] and the potential for $r>b$ is $Ve^{-\xi'(r-b)}/(1-e^{-\xi'(r-b)})$ with $V=-486.3$ Mev and $\xi'=3.20\times10^{13}$ cm^{-1}; for (c) the potential is $V=-35.39$ Mev to a radius of 2.04×10^{-13} cm and 0 for larger radii. The decay parameter $\gamma=(mB/\hbar^2)^{\frac{1}{2}}$ for the deuteron wave function at large r is taken as 0.23166×10^{13} cm^{-1} from the binding energy of 2.226 Mev. (These parameters were kindly furnished by Dr. George Snow.) The calculations for (b) and (c)

[21] Chamberlain *et al.*, reference 18; also Phys. Rev. **95**, 850 (1954), **95**, 1105 (1954), and unpublished work.
[22] L. Wolfenstein, Phys. Rev. **96**, 1654 (1954).
[23] P. B. Daitch and J. B. French, reference in footnote 19.
[24] R. Jastrow, Phys. Rev. **81**, 165 (1951); **81**, 636 (1951).

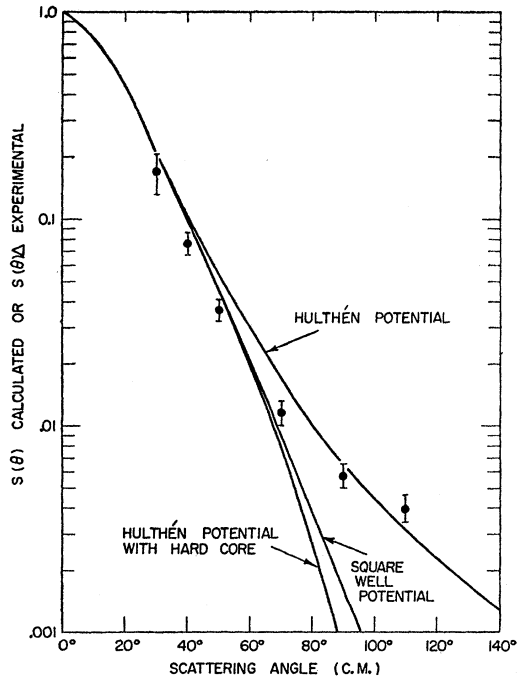

FIG. 9. $S(\theta)$ for three different n-p potentials, the parameters for which are given in text. The points shown are calculated from our p-d results using Eq. (4).

required approximations; the calculations were carried out to a point where the error in S is less than one percent except where S is of the order of 10^{-6} or less.

Table II shows the resulting values of $S(K)$. Also shown in the table are the center-of-mass quantities $K=5.40\sin(\theta/2)\times10^{13}$ cm^{-1} and the corresponding $\Delta p=197K$ in units of Mev/c. These sticking factors are in addition plotted on a semilogarithmic graph in Fig. 9.

The experimental quantity $S(\theta)\Delta$ is included in Fig. 9. For small scattering angles (less than 40°) the value of S seems to depend very little on the n-p interaction chosen. In this region of angles the points derived from the experimental results fall slightly below the calculated curves for S, indicating that Δ is slightly less than 1. This is taken to indicate that there is very little interference or perhaps slightly destructive interference between n-p and p-p scattering at these angles.

TABLE II. The sticking factor S as a function of θ or K for three different n-p potentials (parameters given in text).

θ (deg)	Hulthén	Hulthén with core	Square well	K (in 10^{-13} cm)	Δp (in Mev/c)
20	0.4302	0.4299	0.4285	0.9377	184.6
30	0.2156	0.2100	0.2088	1.3976	275.2
40	0.1079	0.09792	0.09763	1.8469	363.6
50	0.05589	0.04426	0.04490	2.2822	449.3
70	0.01730	0.00800	0.00909	3.0973	609.8
90	0.006616	0.000865	0.001685	3.8184	751.8
110	0.003136	$<10^{-6}$	0.000287	4.4234	870.9
130	0.001791	0.000139	0.000042	4.8941	963.5
150	0.001245	0.000305	5×10^{-6}	5.2160	1026.9

Table III lists the nucleon-nucleon angles and energies required, the values of $\sigma_{np}(\theta')$ and $\sigma_{pp}(\theta')$ obtained by interpolation and extrapolation from experiments at neighboring energies[25] (with errors somewhat arbitrarily assigned) and $(9/16)\sigma_{pd}(\theta)$ as measured in this experiment. The last two columns give, respectively, $2/K\sim r$, and an estimate of the double-scattering probability in the form of the quantity $\sigma_{pp}{}^{\text{total}}/4\pi r^2$.

For angles larger than 50° it is virtually impossible with presently available information to make a direct application of the impulse-approximation theory. As indicated in Fig. 9, the sticking factor S is strongly dependent on the n-p potential interaction chosen, and there remains also the lack of information about the nucleon-nucleon scattering amplitudes. Furthermore, corrections to the impulse approximation may become very important.

TABLE III. Nucleon-nucleon parameters used in Eq. (4). The last two columns show parameters useful in estimating the validity of the impulse approximation.

θ deg.	θ' deg.	T' Mev	σ_{np} mb/sterad	σ_{pp} mb/sterad	$(9/16)\sigma_{pd}$ mb/sterad	r 10^{-13} cm	Probability of double scattering
30	39.5	350	3.40±0.36	3.86±0.15	1.25 ±0.28	1.43	0.087
40	53.5	363	2.69±0.34	3.78±0.15	0.502 ±0.070	1.08	0.16
50	65.0	389	2.35±0.13	3.62±0.15	0.220 ±0.033	0.88	0.23
70	86.0	426	1.73±0.09	3.42±0.15	0.0608±0.0079	0.66	0.41
90	106.5	471	1.10±0.20	3.40±0.15	0.0263±0.0034	0.52	0.67
110	124.4	518	1.90±0.22	4.0 ±0.2	0.0239±0.0026	0.45	0.88

VIII. ACKNOWLEDGMENTS

The authors wish to express their appreciation for helpful discussions with Professor Emilio Segrè. Dr. Clyde Wiegand contributed valuable advice, and portions of the apparatus were designed and constructed by him. To various graduate students go thanks for assistance in construction of some of the equipment and in execution of runs at the cyclotron.

Dr. George Snow of Brookhaven National Laboratory and Professor Robert Serber of Columbia University contributed much to clarification of the interpretation.

We are grateful to Dr. Amos Newton and Professor George Pimentel for the analyses of the target material, to Miss Greta Kemp for reading portions of the film, and to the cyclotron crews directed by Mr. James Vale for providing at all times the proton beam that was desired.

One of us (D.D.C.) wishes to acknowledge indebtedness to the U. S. Atomic Energy Commission for the AEC Predoctoral Fellowship under which a major portion of this work was done.

[25] J. Depangher, University of California Radiation Laboratory Report UCRL-2153 (unpublished); A. J. Hartzler and R. T. Siegel, Phys. Rev. **95**, 185 (1954); Hartzler, Siegel, and Opitz, Phys. Rev. **95**, 591 (1954); Chamberlain *et al.*, reference 9; and W. E. Mott, U. S. Atomic Energy Commission Report NYO-3657 (unpublished).

APPENDIX—KINEMATICS OF INELASTIC SCATTERING

For purposes of comparing the kinematics of the elastic and inelastic events to determine in part the nature of the background produced by inelastic scattering, it is sufficient to use nonrelativistic equations for both processes.

The inelastic kinematics may be handled by an impulse treatment mentioned in Sec. 2. The incident proton is assumed to strike only one nucleon of the deuteron, and the other nucleon is assumed to be unaffected by the collision, maintaining after the collision the same vector momentum it had due to internal motion in the deuteron before the collision. This vector momentum is equal but opposite to the vector momentum of the struck particle at the time of collision, as the deuteron as a whole is at rest. We may therefore write the energy-conservation law as

$$T_1'+T_2'+T_2=T_1-B,$$

where T denotes kinetic energy, the subscripts 1 and 2 refer to the incident and struck particles, respectively, and B is the deuteron binding energy. Primed quantities are postcollision values, and unprimed quantities are precollision ones. The term T_2 on the left side is the kinetic energy carried off by the unstruck particle.

The momentum-conservation law need be applied only to the two nucleons involved in the collision, as the unstruck particle does not suffer any momentum change.

These assumptions have received experimental support (for collisions in which the deuteron internal momentum is not assumed unreasonably large) in the observations of Bloom and Chamberlain[26] in studying 192-Mev d-p inelastic scattering.

We have solved these equations graphically by constructing a laboratory-system momentum diagram, an example of which is shown in Fig. 10. (The example is for a p-d center-of-mass scattering angle of 90°.) As we are most interested in the inelastic events yielding protons emergent in the directions for elastic scattering, we set up a nonrectangular coordinate system whose axes lie along the elastic scattering directions. As the example drawn in dotted lines shows, any point on the page will satisfy the momentum-conservation requirements. The curved line, found by trial and error, shows the locus of those points which also satisfy the energy-conservation law. This curve then shows what momentum range will be covered by the inelastically scattered protons proceeding in the directions of elastically scattered particles. (With some thought, one can also read the qualitative features of the momentum distributions.)

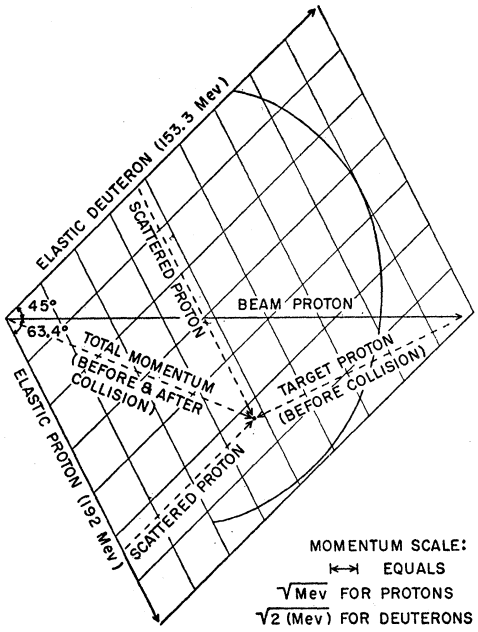

FIG. 10. Momentum diagram (laboratory system) for inelastic scattering observable at elastic-scattering angles. See the appendix for further explanation.

We note in particular that inelastically scattered protons emerging at the deuteron angle have a spectrum of ranges surrounding the deuteron range, and that a few inelastically scattered protons emerging in the direction of an elastically scattered proton have a range almost as great as the latter. These facts lead to the requirement of a detection method that identifies the deuterons.

[26] A. Bloom and O. Chamberlain, Phys. Rev. 94, 659 (1954).